Turkish Journal of Engineering & Environmental Sciences

http://journals.tubitak.gov.tr/engineering/

Research Article

Turkish J Eng Env Sci
(2014) 38: 64 – 78

doi:10.3906/muh-1401-13

DEM resolution and stream delineation threshold effects on the results of geomorphologic-based rainfall runoff models

Asghar AZIZIAN[1], **Alireza SHOKOOHI**[2,*]
[1]Department of Water and Hydraulic Structures, Tehran University, Iran
[2]Department of Water Engineering, Faculty of Engineering and Technology,
Imam Khomeini International University, Qazvin, Iran

Received: 23.01.2014 • **Accepted:** 10.07.2014 • **Published Online:** 24.10.2014 • **Printed:** 21.11.2014

Abstract: Digital elevation model (DEM) resolution and the assigned threshold for river network delineation affect the results of rainfall-runoff models. In this study, the effects of these 2 issues on the extracted geomorphologic parameters of watersheds and the performance of a kinematic wave based model, called KW-GIUH, are investigated. The results show that by decreasing the DEM resolution at fixed thresholds, parameters such as subbasin mean slope and the number of streams decrease and the area of the ith order subbasins and the mean length of the overland flow increase. Moreover, the results indicate that the reduction of the DEM resolution at a fixed threshold causes the peak flow and hydrograph time base to decrease up to the cell size of 100 m and then, after experiencing a jump, again decrease with the increase of the cell size. According to the achieved results, above the threshold of 2%, the difference between the peak flows of different hydrographs at different resolutions is meaningful. The KW-GIUH sensitivity to DEM resolutions and thresholds is sharper in peak flow and then in hydrograph time base and time to peak. At a fixed threshold, the value of time to peak is independent of DEM resolution.

Key words: DEM resolution, KW-GIUH, thresholds, peak flow, hydrograph base time, time to peak

1. Introduction

The main step in rainfall-runoff modeling is extracting the geomorphological parameters of watersheds. For this purpose, digital elevation models (DEMs) are widely used to delineate watershed, define drainage divides (watershed boundaries), and identify stream networks [1]. DEMs and their related algorithms like flow tracing have been widely considered in recent years [2]. The accuracy of extracted data from DEMs is highly dependent on DEM cell size [3]. Although DEMs cell sizes (DEM resolution) affect the extracted data and consequent analysis quality, there are limited studies that address the effects of DEM cell size in rainfall-runoff modeling and extracting watersheds geomorphological parameters [4–7]. Using DEMs with small cell sizes does not guarantee the correct performance of rainfall-runoff models. With respect to different results of such models using high-resolution DEMs in various catchments, one could deduce that selecting the optimum resolution is complicated and needs to be investigated. Increasing DEM resolution (i.e. decreasing cell size) increases the accuracy of data obtained from DEMs, but on the other hand it increases the data volume, which could make trouble for computer memory allocation and data management. On the contrary, while decreasing DEM resolution (i.e. increasing cell size) reduces data volume, by decreasing the information content of the data, it could cause error in the extracted geomorphological parameters and then in the results of rainfall-runoff model.

*Correspondence: shokoohi@eng.ikiu.ac.ir

McMaster evaluated the effect of DEM resolution on the accuracy of extracted stream network. He used DEMs with 30- to 3000-m resolution to compare the extracted stream network with that obtained from DEMs based on topographic maps [8]. Results showed that by decreasing the DEMs' resolution from 150 to 3000 m, the accuracy of extracted stream network and the number of streams of orders 1 and 2 were decreased. Hancock studied the effect of DEM resolution on the geomorphological features of 2 catchments of different climates in Australia [9]. He could illustrate the dependence of slope–area relationship and also the stream ordering scheme on DEM resolution, while the hypsometric curve of the 2 watersheds showed a low sensitivity to changing DEM resolution. Studies on the Soil and Water Assessment Tool (SWAT) conducted by Chaubey et al. indicated that the effect of DEM resolution on extracted stream network, number of subbasins, and formation of hydrologic response unit was considerable [10]. Smith et al. assessed the effect of DEM resolution on the soil erosion at several catchments in the United States [11]. Results indicated that employing high-resolution DEMs does not mean that one could achieve a more accurate estimation of soil erosion, and the required resolution for modeling is related to the goal and the type of study. Pradahan et al. applied TOPMODEL to evaluate the effect of DEM resolution on the simulation of runoff in the Kamishiba catchment, Japan [12]. They found that based on using a DEM of 50-m resolution only 7% of the catchment contributes in the runoff generation, while using a DEM of 1000-m resolution increases this percent to 59%. Lin et al. investigated the effect of DEM resolution on the simulated surface runoff by SWAT model in the Xiekenggxi catchment in China [13]. Results showed that the simulated runoff by SWAT is not sensitive to DEM resolution. Nourani and Zanardo, by employing a wavelet-based DEM regularization methodology, could improve the performance of a distributed rainfall-runoff model in different DEM resolutions. This method increases the connection of saturated areas and subsequently enhances the performance of the model in different cell sizes [14]. Nourani et al. investigated the effects of different time scales and different flow tracing algorithms on the performance of TOPMODEL. Results showed that the simulated hydrograph using the D_{inf} algorithm was more accurate than the D_8 algorithm, especially in event-based modeling [15].

The goal of the current study is to analyze the effect of DEM resolution and the thresholds of stream network delineation on the performance of a specific type of rainfall-runoff models. The model used in this study is the kinematic-wave-based geomorphologic instantaneous unit hydrograph (KW-GIUH), which is a conceptual rainfall-runoff model and uses the geomorphological instantaneous unit hydrograph to simulate floods. The reason for using this model is the importance of the geomorphologic parameters in the model structure that ascertain a reliable comparison between the effects of DEM resolution and the thresholds of streams' definitions on the model performance.

2. Materials and methods

2.1. Structure and required parameters of the KW-GIUH model

Overland flow over a permeable surface can occur when the rainfall intensity is greater than the infiltration capacity or when surface saturation exists in regions near the stream [16]. When a unit depth of excess rain falls uniformly and instantaneously onto a catchment, the unit excess rainfall is assumed to consist of a large number of independent, noninteracting raindrops. Thus, the whole rainfall-runoff process can be represented by tracing the excess rainfall moving along different paths towards the catchment outlet to produce the outflow hydrograph [17]. Based on the Strahler stream-ordering method, a catchment of order Ω can be divided into different states. Most of the surface flow occurs on the low portions of the catchment; after that, it goes into the adjacent channel and then flows through the stream network to the outlet. Each raindrop falling on the

overland region will move successively from lower to higher orders of channels until it reaches the outlet. The catchment geomorphology is represented probabilistically based on the stream order, instead of simulating the overland surfaces and channels by their individually actual geometry as in the deterministic modeling [17]. An ith order overland region is denoted by x_{oi} while x_i represents the ith order channel, where i =1,2,..., Ω. If w denotes a specified runoff path: $x_{oi} \rightarrow x_i \rightarrow \ldots\ldots \rightarrow x_\Omega$, the probability of a drop of rainfall excess adopting this path can be expressed as:

$$P(w) = P_{OAi} P_{x_{oi}x_i} \ldots . P_{x_i x_j} \ldots . P_{x_k x_\Omega}, \tag{1}$$

where $P_{x_{oi}x_i}$ is the transitional probability of the raindrop moving from the ith order overland region to the ith order channel and $P_{x_i x_j}$ is the transitional probability of the raindrop moving from the ith order channel to a jth order channel and is computed as:

$$P_{x_i x_j} = \frac{N_{i,j}}{N_i}. \tag{2}$$

Here, $N_{i,j}$ is the number of ith order channels contributing to the jth order channels, and P_{OAi} is the ratio of the ith order overland area to the total catchment and is computed as:

$$P_{OAi} = \frac{1}{A}\left(N_i \bar{A}_i - \sum_{i=1}^{i-1} N_i \bar{A}_i P_{x_i x_j}\right), \tag{3}$$

where $\bar{A}_i$ is the mean area of the ith order channels and is estimated as:

$$\bar{A}_i = \frac{1}{N_i}\sum_{j=1}^{N_i} A_{ij}. \tag{4}$$

It should be noted that A_{ij} denotes not only the areas of the overland flow regions that drain directly into the jth order, but it also includes all upstream overland areas drained into the lower order channels finally terminating at this jth channel of order i. It is assumed that the exponential distribution can be used to simulate the travel time of overland flow and also the storage component of the channel, but the translation component of a channel is assumed to follow a uniform distribution. For the state x_k, the travel time of the channel storage component and channel translation component are $T_{x_{rk}}$ and $T_{x_{ck}}$, respectively, and the total travel time is $T_{x_k} = T_{x_{rk}} + T_{x_{ck}}$.

The instantaneous unit hydrograph can be represented by the convolution of 2 groups of the probability density functions and is given by:

$$u(t) = \sum \left(\left[f_{x_{oi}}(t) * f_{x_{ri}}(t) * f_{x_{rj}}(t) * \ldots . * f_{x_{r\Omega}}(t)\right] * \left[f_{x_{ci}}(t) * f_{x_{cj}}(t) * \ldots .. * f_{x_{c\Omega}}(t)\right]\right).P(w). \tag{5}$$

The first part of Eq. (5) represents the overland flow region (x_{ok}) and the channel storage component (x_{rk}). The exponential distribution with a mean travel time of T_{x_k} is:

$$f_{x_k}(t) = \frac{1}{T_{x_k}} exp?(-\frac{t}{T_{x_k}}). \tag{6}$$

The second part of Eq. (5) represents the channel translation component (x_{ck}). The uniform distribution with a mean travel time of T_{x_k} over an interval of $(0,\ 2T_{x_k})$ is:

$$f_{x_k}(t) = \begin{cases} \frac{1}{2T_{x_k}} & 0 \le t \le 2T_{x_k} \\ 0 & otherwise \end{cases}. \tag{7}$$

The distribution function bound is set to be from 0 to $2T_{x_k}$ because of the definition of the mean travel time. Substituting in the previous equation, the instantaneous unit hydrograph can be expressed analytically as:

$$u\left(t\right)=\sum_{w\epsilon W}\{\frac{1}{T_M}[G\left(t\right)+\sum_{k=1}^{N_w}\left(-1\right)^k U_{2T_{x_M}}\left(t\right)G(t-2T_{x_M})]\}_w.P(w)\,, \tag{8}$$

where $U_c\left(t\right)$ is a unit step function [$U_c\left(t\right)=1$ for t$\geq$0, and $U_c\left(t\right)=0$ for t$<$c], N_w is the total number of different order channels in the path w, and

$$T_m=T_{x_{oi}}T_{x_{ri}}T_{x_{rj}}\ldots T_{x_{r\Omega}}\left(2T_{x_{ci}}\right)\left(2T_{x_{cj}}\right)\ldots\left(2T_{x_{r\Omega}}\right), \tag{9}$$

$$G\left(t\right)=a_1+a_2t+\ldots+\frac{1}{(N_w-1)!}a_{N_w}t^{N_w-1}+b_{oi}exp\left(-\frac{t}{T_{x_{oi}}}\right)+c_iexp\left(-\frac{t}{T_{x_{ri}}}\right)+c_jexp\left(-\frac{t}{T_{x_{rj}}}\right)+\cdots+c_\Omega exp\left(-\frac{t}{T_{x_{r\Omega}}}\right), \tag{10}$$

$$X_M=\{x_{ci},x_{cj},\ldots,x_{ck}\}\,\epsilon x_{ci}x_{cj},\ldots,x_{ck},\ldots,x_{c\Omega}, \tag{11}$$

$$T_{x_M}=\sum_{i=1}^{M}T_{x_{ci}}, \tag{12}$$

where M denotes the size of X_M and a_1, $a_2,...,a_{N_w}$, b_{oi}, c_i, $c_j,...,c_\Omega$ are coefficients. The coefficients are determined by comparing coefficients in partial fractions after applying the Laplace transformation.

Finally, Lee and Yen, by using kinematic-wave approximation and a simplified V-shaped model first introduced by Wooding [18], derived travel-time equations for different orders of overland regions and channels. The runoff travel-time for a specified flow path can be estimated as [17]:

$$T_w=T_{oc_i}+\sum_{k=i}^{\Omega}T_{cc_k}=\left(\frac{n_o.\bar{L}_{oi}}{\bar{S}_{oi}^{0.5}.i_e^{m-1}}\right)+\sum_{k=i}^{\Omega}\frac{B_k}{2\,\bar{i}_e\,\bar{L}_{o_k}}\left[\left(h_{co_k}^m+\frac{2\,.i_e\,.n_c.\bar{L}_{o_k}.\bar{L}_{c_k}}{\bar{S}_{c_k}^{0.5}.B_k}\right)^{1/m}-h_{co_k}\right], \tag{13}$$

where T_w is the runoff travel-time for a specified flow path w; T_{oc_i} is the mean travel-time on the ith order overland planes; T_{cc_k} is the mean travel-time in the kth order channels; $\bar{L}_{oi}$ is the mean length of the ith order overland flow; $\bar{L}_{c_k}$ is the mean length of the kth order channel; i_e is the excess rainfall intensity; $\bar{S}_{oi}$ is the mean slope of ith order overland flow; $\bar{S}_{c_k}$ is the mean slope of kth order channel; B_k is the width of the kth order channel; Ω is the stream order at the outlet; n_o and n_c are the roughness coefficients for overland flow areas and channels, respectively; and h_{co_k} is the inflow depth of the kth order channel. The runoff structure of a simplified V-shaped model is shown in Figure 1.

In the above equation, the value of h_{co_k} is equal to 0 for k = 1 because no channel flow is transported from upstream. For $1<\mathrm{k}<\Omega$, h_{co_k} can be expressed as [17]:

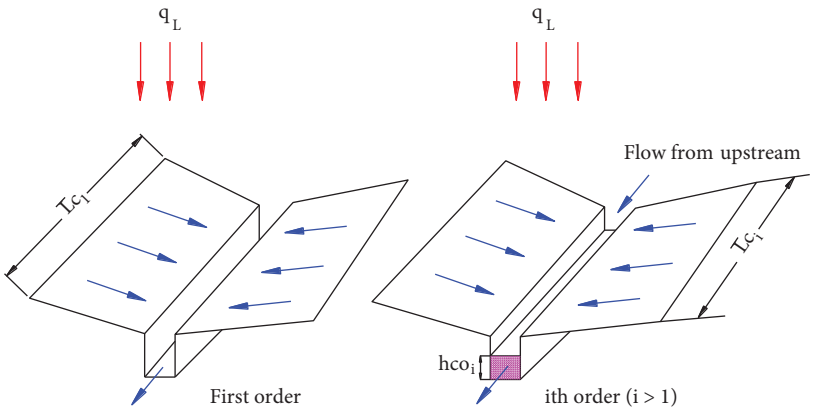

Figure 1. V-shaped subbasins (from Wooding [18]).

$$h_{co_k} = \left(\frac{i_e . n_c \left(N_k . \bar{A}_k - A\, P_{oA_k} \right)}{N_k . B_k . \bar{S}_{c_k}^{0.5}} \right)^{\frac{1}{m}}, \tag{14}$$

where N_k is the number of kth order channels and $\bar{A}_k$ is the mean area of the kth order subbasins. As shown in Eq. (13), a number of geomorphologic factors are required to estimate the runoff travel-time on overland regions and in channels that can be easily obtained from a DEM.

The values of overland and channel roughness can be estimated by field investigation (from the overland or channel hydraulic properties) or can be determined by tabular data introduced in the literature like what was presented by Chow [19] and Usul and Yılmaz [20]. To simplify field investigation works, the relationship between channel width and catchment area is given as [21]:

$$B_k = B_\Omega \left(\frac{\bar{A}_k}{A} \right)^{0.5}, \tag{15}$$

where, B_k is the kth order channel width, B_Ω is the channel width at the catchment outlet, $\bar{A}_k$ is the mean of the drainage area of order k, and A is the total catchment area.

2.2. Preprocessing of DEMs and extracting the stream network

A sink is a set of cells with the same height that may cause error in flow tracing by creating holes in DEMs. In fact, they cause loss of flow by breaking DEM cells' connectivity. Therefore, sinks have to be removed before extracting the stream network and other required parameters for the KW-GIUH model. This preprocess is required to increase the accuracy of DEMs and guarantee the model performance. Sinks mainly appear in narrow valleys, where the valley's width is less than the cell size. Moreover, because of interpolation errors, sinks might appear in low-slope areas. The Archydro extension embedded in ArcView GIS is a common tool for sink elimination. After this step, a flow direction grid is extracted for each cell of the DEM. By using the flow direction grids, the flow accumulation network for each cell could be derived. In a flow accumulation network, the value of each cell represents the number of total cells drained into it. In this study for a DEM of 50-m resolution, the flow direction grid and flow accumulation network are extracted by using the D_8 algorithm (the flow tracing algorithm in the Archydro extension). In the flow accumulation network, cells with the highest accumulation represent streams and the cells with a value of 0 match the watershed boundaries. To extract

artificial stream network from a flow accumulation map, it is necessary to determine precisely a threshold, which is the percent of watershed total cells poured into the target cell. Choosing a low threshold leads to a high number of streams (smaller subbasins), and, on the contrary, choosing a high threshold will generate a small number of streams (larger subbasins). The bench mark of the threshold value is the value of 1%. In some GIS extensions such as Archydro and HEC-GeoHMS, the default value for stream delineation threshold is 1% of catchment area or 1% of maximum flow accumulation grid. Furthermore, the minimum area for starting streams is equal to 1% of the maximum value of flow accumulation grid (which is located at the catchment outlet). Therefore, focusing on this value, the thresholds of 0.25%, 0.5%, 1%, 2%, and 3% were employed for the extraction of stream network. Furthermore, DEMs with different resolutions (25, 50, 75, 100, 200, and 300 m) were constructed using a topographic map (with a scale of 1/25,000 and 25-m intervals between contour lines) and, eventually for each threshold, the stream networks and other geomorphological parameters were extracted.

2.3. Study area

The study area is the Kasilian watershed, a small part of the Caspian Sea watershed and considered as 1 of the 6 major watersheds in Iran. The Kasilian watershed has an area of 67 km^2 and a perimeter of 37.8 km; it is drained by the Kasilian River with a length of 17 km. The average slope of this watershed is 16.4%, and its elevation ranges between 1100 and 2650 m above sea level. The location of Kasilian watershed and its DEM map with 50-m resolution are shown in Figure 2. The Valikbon hydrometric station, at X = 53°06′ and Y = 36°01′, is located at the watershed outlet and has been operated by the Mazandaran Regional Water Board since 1975.

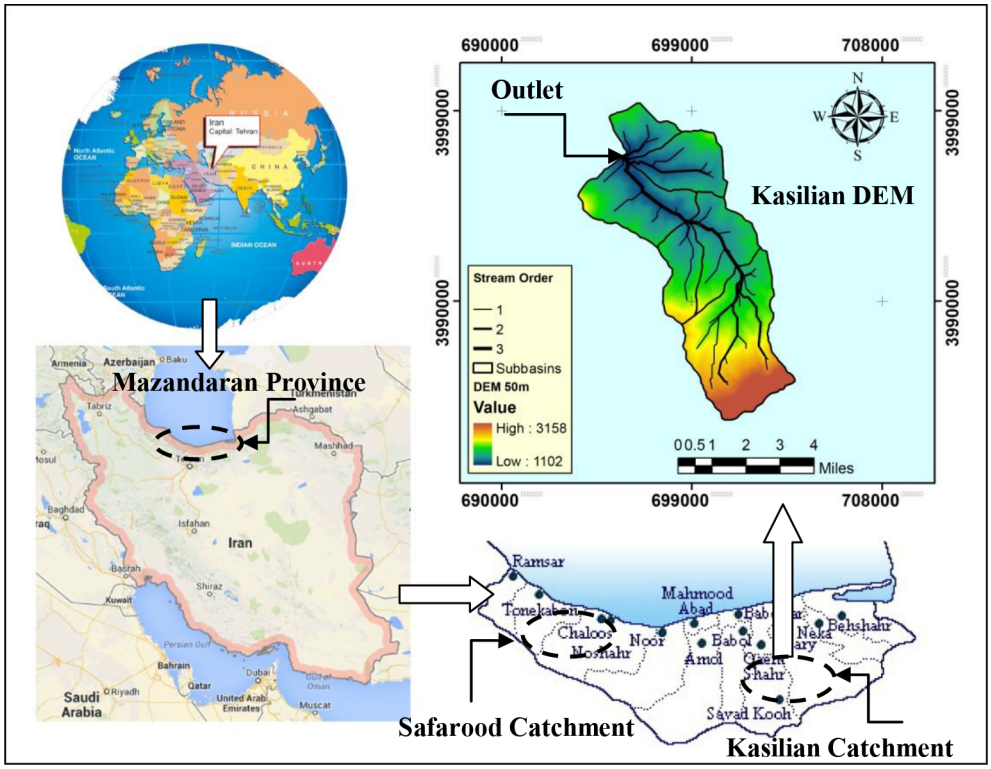

Figure 2. Kasilian watershed location, 50-m DEM, and its main streams.

2.4. Hydrographs and the data used for calibration and verification of the model

To analyze the KW-GIUH performance in the Kasilian watershed, hydrographs recorded at the Valikbon hydrometric station were used. In this gauge station, there are just 4 reliable recorded hydrographs, 2 of which (occurred 1991/03/28 and 1987/10/09) are used for model calibration and 2 of which (occurred 2005/11/09 and 1993/09/03) are employed for model verification. In the present study, the values suggested by Usul and Yılmaz [20] are used to confirm the results achieved from field investigation. The values of the overland and channel roughness for the Kasilian catchment are 0.6 and 0.3, respectively. In this study, based on the field investigation, the channel width at the catchment outlet was obtained as about 32 m, and based on Eq. (15) the widths of other streams (of different orders) were calculated.

The only important parameter of the KW-GIUH model required to be calibrated is the infiltration rate. In this model, the ϕ index is used for calculating net rainfall.

3. Results and discussion

3.1. The geomorphological parameters required for the model

The geomorphological parameters of the study area are presented in Table 1.

Table 1. Geomorphological properties of the Kasilian River basin.

Catchment mean elevation (m)	Mean channel slope (%)	Gravel ratio	Longest channel length (km)	Perimeter (km)	Area (km^2)
1569	4.7	1.3	17.2	37.8	67

In this study, to derive the geomorphological parameters of watershed, the thresholds of 0.25%, 0.5%, 1%, 2%, and 3% and DEM with cell sizes of 15, 25, 50, 75, 100, 150, 200, and 300 m were used. Because of the high volume of extracted data, only the geomorphological parameters at the thresholds of 0.25% and 3% (with different DEM cell sizes) are shown in Figures 3–8.

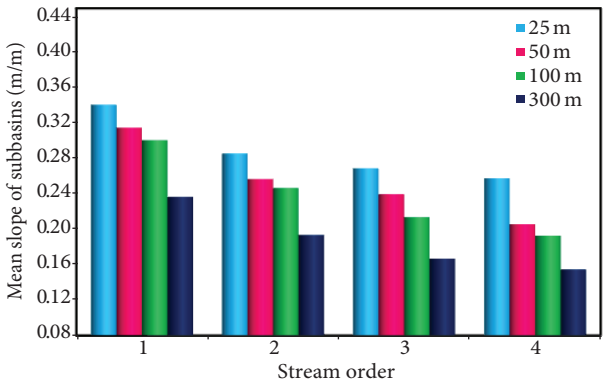

Figure 3. Variation of the mean slope of the ith order subbasins at different cell sizes (at threshold of 0.25%).

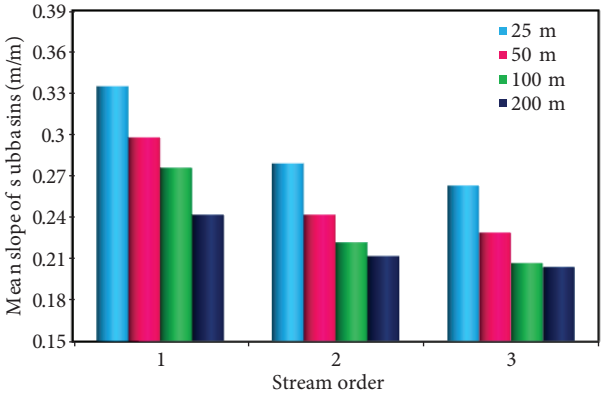

Figure 4. Variation of the mean slope of the ith order subbasins at different cell sizes (at threshold of 3%).

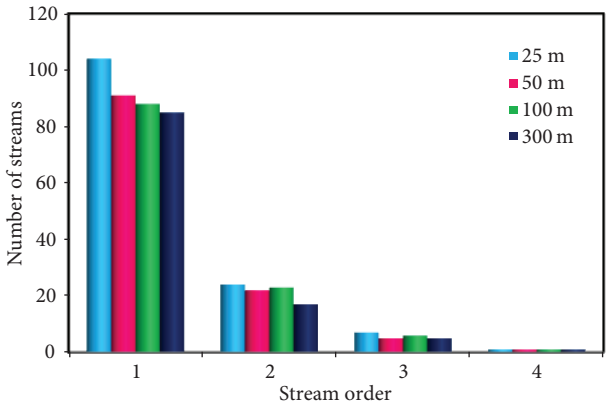

Figure 5. Variation of stream numbers at different cell sizes (at threshold of 0.25%).

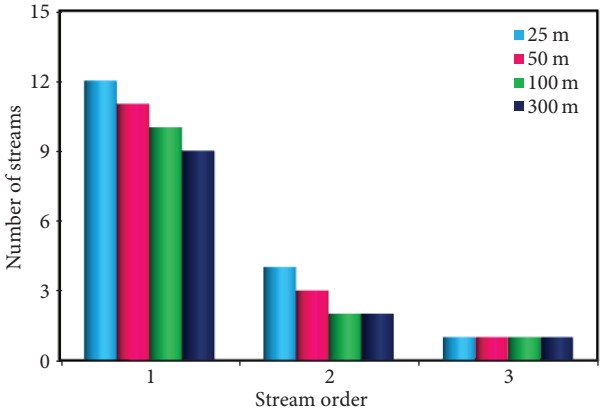

Figure 6. Variation of stream numbers at different cell sizes (at threshold of 3%).

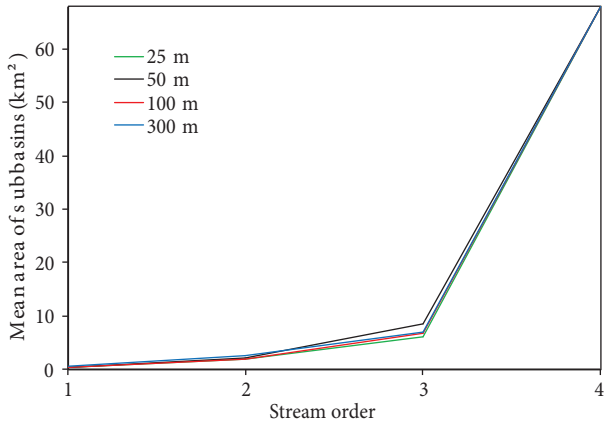

Figure 7. Variation of the mean area of the ith order subbasins at different cell sizes (at threshold of 0.25%).

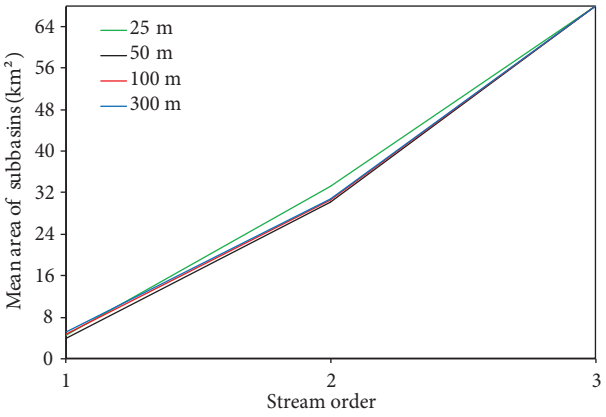

Figure 8. Variation of the mean area of the ith order subbasins at different cell sizes (at threshold of 0.25%).

Results show that by decreasing the DEM resolution, the mean slope of the ith order subbasins decreases. Reducing the subbasins slope leads to the increase of the travel-time of the overland flow and hydrograph time base, and this in turn decreases the hydrograph peak flow. It seems that the mean slope of the ith order subbasins is one of the most important and sensitive parameters of the KW-GIUH model that could have a significant effect on the shape and other important parameters of the simulated hydrograph. Additionally, the results indicate that by increasing the DEM resolution, the number of streams increases (Figures 5 and 6). Increasing of the number of streams of orders 1 and 2 is greater than that of the other orders (there is no significant difference between the number of streams of orders 3 and 4). Decreasing the number of streams in low-resolution DEM (using greater cell size) will decrease the drainage density and hydrograph peak flow and subsequently increase the hydrograph time base. The mean area of ith order subbasins is also one of the effective parameters regarding the model performance. Nonetheless, as shown in Figures 7 and 8, the effect of DEM resolution on this parameter is not considerable and its trend of variation is almost identical at all thresholds. According to the achieved results, it can be said that the effect of DEM resolution on geomorphological parameters of the KW-GIUH model is considerable. Therefore, it is necessary to evaluate the effects of the above parameters' variation due to using different DEM resolutions and thresholds on the

KW-GIUH model performance. The next sections are devoted to the investigation of the model performance under variable basic parameters.

3.2. Model calibration and verification

One of the strong and valuable points of the KW-GIUH model, like all other geomorphological models, is the fact that the model obtains most of its parameters from catchment geomorphological properties and therefore there is little need for calibration. The most important parameter of the model required to be calibrated is the infiltration rate. In this model, the Φ index is used to estimate the infiltration rate during rainfall and can be calculated with the help of recorded hydrographs. A trial-and-error procedure is used to calibrate the model by implementing different infiltration rate values (Φ) in the model until the resulted hydrograph is nearly equal to the recorded hydrograph. In Figure 9, the results of the calibration and verification of the model are shown. The model efficiency based on the Nash–Sutcliffe method is presented in Table 2.

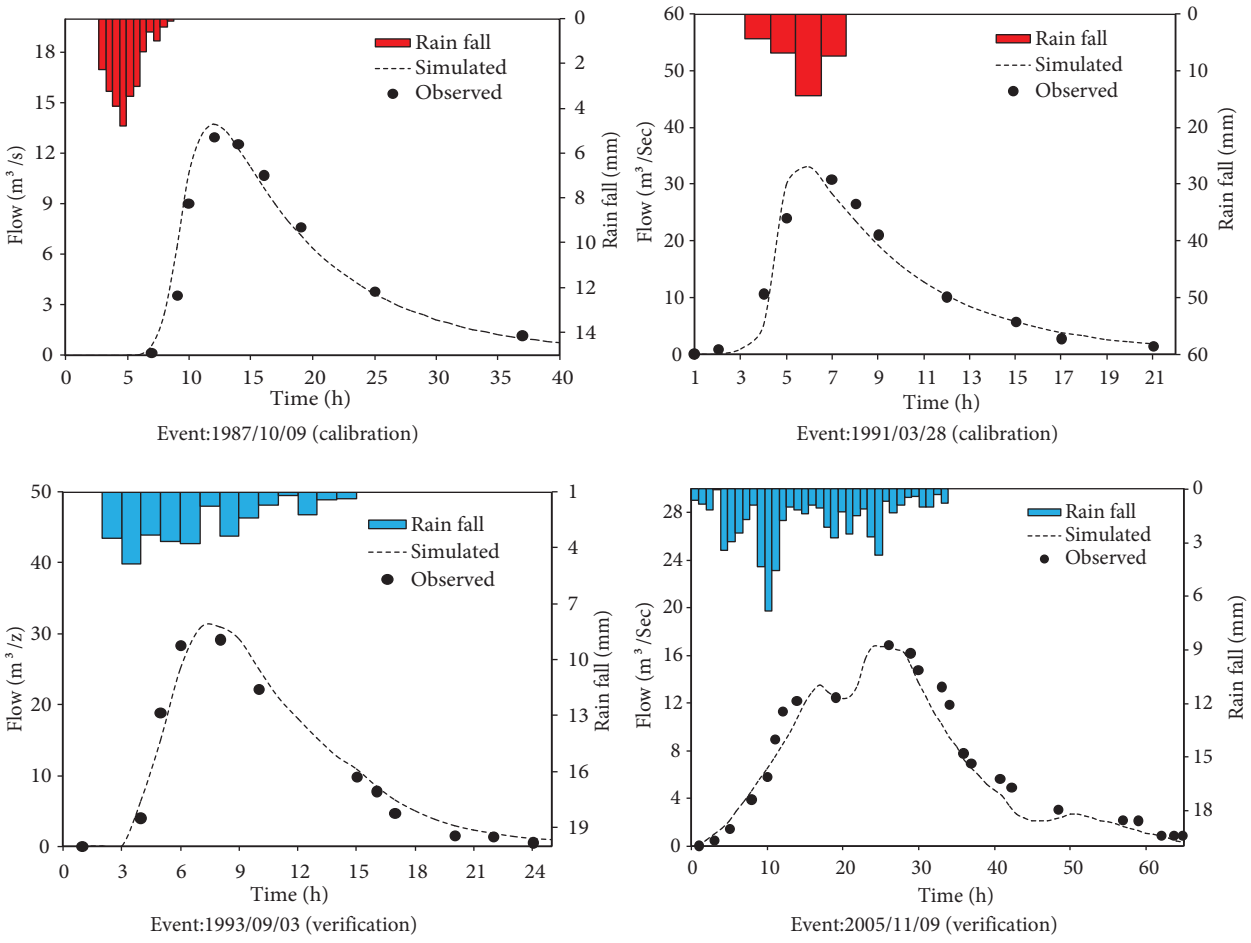

Figure 9. Observed and simulated hydrographs of events at calibration and verification steps.

As is seen in Table 2 and Figure 9, the model results, both in the calibration and the verification phases, show good agreement with the observed data and indicate the acceptable performance of the KW-GIUH in simulating the rainfall-runoff process of the Kasilian watershed.

Table 2. The results of calibration and verification phases of storm events.

Storm event	Phase	Nash–Sutcliffe efficiency
1991/03/28	Calibration	0.91
1987/10/09		0.88
2005/11/09	Verification	0.83
1993/09/03		0.86

3.3. The effect of threshold on the model performance

In this study, to extract the stream network and other geomorphological parameters, while keeping the DEMs' resolution constant, the thresholds of 0.25%, 0.5%, 1%, 2%, and 3% are employed to analyze the model performance. The results indicate that the simulated peak flow is adversely affected by changing the thresholds; that is, peak flow increases by decreasing the threshold and decreases when the threshold is increased. Additionally, at low thresholds, the base time and the time to the peak of the hydrograph decrease. One of the most important issues for a flood warning system is time to peak, which, according to the results, could be influenced by the selection of the threshold.

The model's results show its sensitivity to peak flow, time to peak, and hydrograph base time. The model has a maximum sensitivity to the peak flow, and then to the base time, while time to peak has a minimum influence on its performance. The simulated peak flow at the threshold of 0.25% shows a difference of 67% with the simulated peak flow at the threshold of 3%. Furthermore, the base time and the time to peak at the threshold of 3% are respectively 17 h and 1 h greater than at 0.25%. Figure 10 shows the effect of different thresholds on the form and peak flow of the simulated hydrograph.

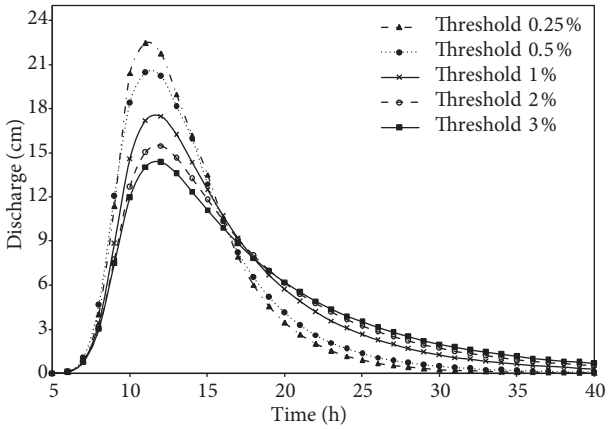

Figure 10. The effects of threshold variations on the simulated hydrograph (at 50-m DEM; event 1987/10/09).

The slope of the hygrograph's rising limb is sensitive to the decreasing/increasing of thresholds. As is seen in Figure 10, the rising limb's slope at a threshold of 0.25% is 1.6 times the rising limb for a threshold of 3%.

Actually, by increasing the stream's formation threshold, the number of extracted streams will be decreased. For example, in the studied watershed, the number of streams of order 1 at a threshold of 0.25% is 91, while at a threshold of 3% it is equal to 11. From a hydraulic point of view, increasing the threshold could increase the contribution of overland in the total flow, where the resistance to flow is increased. Henceforth, regarding the governing equations in uniform flow such as the Manning equation, the flow discharge at each

subbasin could be reduced, which will eventually decrease the simulated hygrograph's peak flow. By applying the same amount of effective rainfall at all states and with respect to the principle of mass balance, the hygrograph base time will increase. Similarly, by increasing the number of first order streams the effective rainfall will spend less time in each subbasin and after arriving into the stream could move at a higher speed toward the watershed outlet. This phenomenon could reduce the time to peak and increase the slope of the hygrograph's rising limb.

3.4. The effect of DEM resolution on the performance of the KW-GIUH

DEM cell size is one the most important parameters that affect the performance of drainage network extraction algorithms. Some researchers indicated that the increase of DEM cell size would lead to the change of the values ??of extracted geomorphologic parameters. For example, Zhang and Montgomery [22] and Wolock and Price [23] showed that by increasing the cell size of a DEM, the slopes of corresponding cells and basins are decreased. As was mentioned, the KW-GIUH model depends on parameters such as mean slope of subbasins, mean slope of channels, mean length of channels, and area of subbasins. Therefore, changing DEM resolution, by affecting the geomorphological parameters, could influence the model performance. In this study, DEMs with different cell sizes (15, 25, 50, 75, 100, 150, 200, and 300 m) are used to investigate the effect of DEM resolution on the simulated hydrograph shape and peak flow.

3.4.1. Hydrograph peak flow

The simulation of hydrograph is performed in 5 steps. At each step, for determining the effects of DEM resolution on the performance of the KW-GIUH model, the threshold for stream delineation is kept fixed, and then for different resolutions (cell sizes), geomorphological parameters are calculated. In Table 3, the results of model simulation at different thresholds and resolutions are presented.

Table 3. Effect of DEM resolution on simulated hydrograph peak flow (for all thresholds).

Threshold (%)	DEM cell size (m)							
	15	25	50	75	100	150	200	300
0.25	23.04	22.66	21.36	20.53	22.45	22.30	22.10	22.02
0.5	19.73	18.95	17.95	17.62	20.45	20.00	19.30	19.00
1	17.84	17.75	17.70	17.60	17.48	17.36	17.21	16.96
2	15.87	14.85	13.74	13.10	15.47	15.21	14.23	14.06
3	15.5	13.77	12.79	12.54	14.35	14.03	12.96	12.76
Difference between peak flows at thresholds of 0.25% and 3%	48.7	64.6	67.0	63.7	56.4	58.9	70.5	72.6

The effect of different DEM resolution on the peak flow is obvious in Table 3. For example, at a threshold of 3%, the maximum and minimum peak flow occur at 15- and 75-m cell sizes, respectively, and their difference is about 26%. The results show that the trend of variation of the peak flow versus the DEM resolution is almost the same for all thresholds. As seen in Table 3 and Figure 11, the reduction of the DEM resolution up to the cell size of 100 m causes the peak flow and hydrograph time base to decrease, and again after experiencing a jump, they decrease with the increase of the cell size. To check the generality of the jump point (at the cell size of 100 m), a large catchment with an area of 420 km^2 (the Safarood river basin located in the west of Mazandaran Province, Iran) was used. The results achieved from this catchment indicate that the jump occurs at a range of

cell sizes of about 80–90 m, which is close to the value obtained in the Kasilian catchment. In Figures 11 and 12, the effects of DEM resolution on the peak flow in the Kasilian and Safarood catchments are shown.

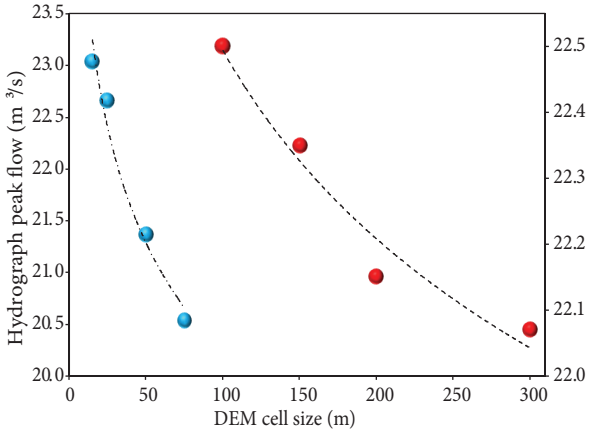

Figure 11. Variation of peak flow and DEM resolution in Kasilian catchment (threshold 0.25%; event 1987/10/09).

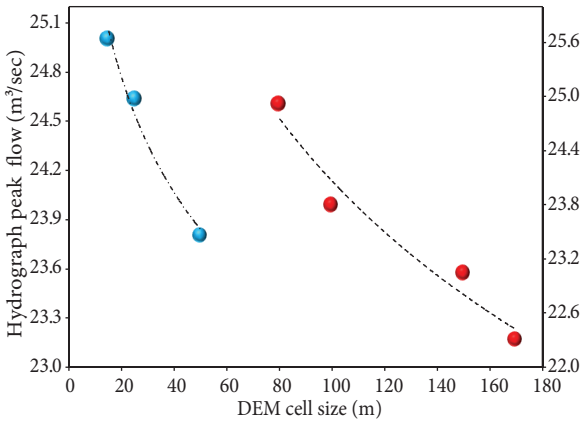

Figure 12. Variation of peak flow and DEM resolution in Safarood catchment (threshold 0.25%; event 1987/10/09).

The occurrence of this jump could be attributed to the abrupt changes of catchment geomorphological parameters when DEM cell size reaches the range of 80–100 m. The critical cell size for the Kasilian watershed is about 100 m. Figures 13 and 14 illustrate the variation of the mean length of the ith order channel against the mean area and the slope of ith order subbasins in DEMs with different cell sizes. As shown in Figure 13, the behavior of mean length of the ith order channel against the mean slope of the ith order subbasin at the cell size of 100 m is different from that of the cell sizes of 25 and 200 m. Additionally, as illustrated in Figure 14, for the mean lengths greater than 3 km and up to 8 km, there are no data for the trend of variation of length against area extracted from DEMs with the cell sizes of 25 and 200 m, while this trend remains linear for the DEM with the cell size of 100 m. Obviously, the subbasin area obtained from the DEM with this cell size is always less than that of other alternatives.

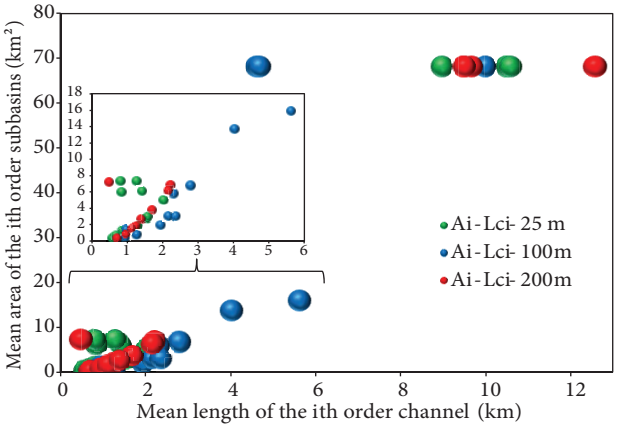

Figure 13. Variation of the mean slope of the ith order subbasins against the mean length of the ith order channel.

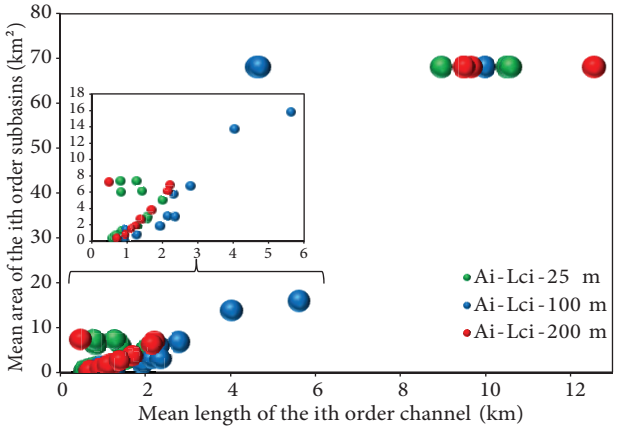

Figure 14. Variation of the mean area of the ith order subbasins against the mean length of the ith order channel.

However, the achieved result in relation to the jumping point is an open area for study and could be a subject for further investigation.

3.4.2. Time to peak and time base of hydrograph

In addition to hydrograph peak flow, estimating its time to peak and base time are important in flood control systems and collection of surface water. In this section the effects of DEM resolution on hydrograph peak flow, time to peak, and time base are studied. The effects of DEM resolution on time to peak and time base are represented in Table 4. The effects of DEM resolution on peak flow and hydrograph shape are shown in Figures 15 and 16 at thresholds of 0.25% and 3%, respectively.

Table 4. Effect of DEM resolution on time to peak and time base (for all thresholds).

DEM cell size (m)	Threshold 0.25%		Threshold 1%		Threshold 2%		Threshold 3%	
	T_{peak}	T_{base}	T_{peak}	T_{base}	T_{peak}	T_{base}	T_{peak}	T_{base}
15	11	50	12	69	12	77	12	78
25	11	52	12	71	12	78	12	79
50	11	56	12	75	12	79	12	81
100	11	54	12	72	12	77	12	80
200	11	59	12	73	12	81	12	81
300	11	60	12	79	12	82	12	82

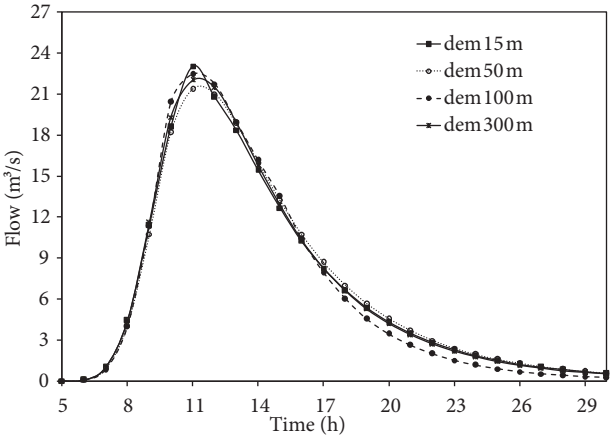

Figure 15. Effect of DEM resolution on peak flow and hydrograph shape at a threshold of 0.25% for event 1987/10/09.

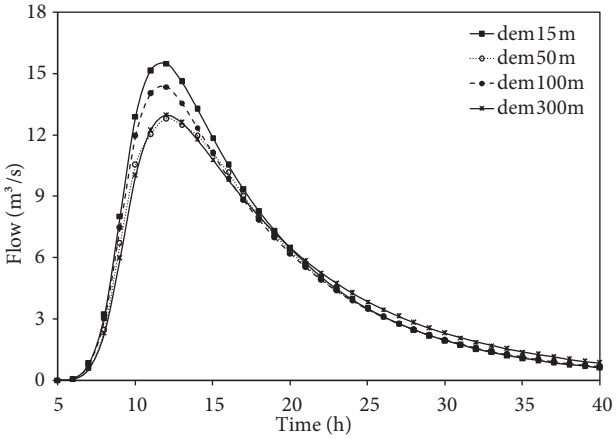

Figure 16. Effect of DEM resolution on peak flow and hydrograph shape at a threshold of 3% for event 1987/10/09.

The results show that decreasing DEM resolution (increasing DEM cell size) increases the hydrograph time base. Again, there is a break point in this trend at the cell size of 100 m. As was noted previously, at this cell size the peak flow experiences a rapid jump. In this situation and by keeping a constant rate of effective rainfall, the base time should be decreased to preserve the principle of mass balance. Table 4 shows that the effects of threshold on the hydrograph base time are more than those of DEM resolution. The maximum difference between time bases at different thresholds is about 28 h for the cell size of 15 m, while the maximum difference between time bases at different DEM resolutions is about 10 h at the thresholds of 0.25% and 1%. The

results indicate that for thresholds higher than 0.5% the time to peak is constant regardless of DEM resolution, but for thresholds lower than 0.5%, the time to peak decreases. In other words, at a fixed threshold the time to peak is independent of DEM resolution.

4. Conclusions

One of the methods used for flood estimation, especially in ungauged watersheds, is employing models that are based on catchments' geomorphological parameters such as the geomorphological instantaneous unit hydrograph (GIUH) and KW-GIUH models. It would be beneficial for researchers to see the effect of DEM resolution on the performance of geomorphological-based models such as KW-GIUH and GIUH. The results obtained in this study showed that the KW-GIUH model is very sensitive to DEM resolution and stream delineation threshold. In this study, regarding the dependence of the KW-GIUH model on catchment geomorphological parameters, the effects of different thresholds and DEM resolution on the geomorphological parameters and model performance were investigated. In comparison to other conceptual rainfall-runoff models, the calibration process of this model is simple and just one parameter must be calibrated. The results of the calibration and verification phases showed reasonable ability of the model to estimate the peak flow and the shape of hydrograph. Investigating the effect of DEM resolution on the geomorphological parameters indicated that by decreasing the DEM resolution the mean slope of the ith order subbasins and the number of streams (especially streams of orders 1 and 2) decrease and the mean area of the ith order subbasins and the mean length of the ith order overland flow increase. The results indicated that by increasing the thresholds, the peak flow decreases while the time base increases. The main reason for this is the fact that by increasing the thresholds the number of streams of order 1 is increased, which in turn decreases the mean length of overland flow and rain-drop travel time. The model's sensitivity to changing DEM resolution and thresholds was sharper in peak flow and then in hydrograph time base and time to peak. For example, using a DEM with 50-m resolution, the simulated peak flow at the threshold of 0.25% was about 67% greater than the peak flow achieved at the threshold of 3%. Evaluation of DEM resolution effect showed that the reduction of the DEM resolution at a fixed threshold causes the peak flow and hydrograph time base to decrease up to the cell size of 100 m. At this resolution the trend experiences a positive jump, after which one can again observe a decreasing trend. Occurrence of this jump point could be related to the variation of catchment geomorphological parameters at the range of about 80–100 m. The results indicated that the maximum difference between the time bases at different DEM resolution was about 10 h. Generally, it can be deduced that the effects of threshold on peak flow and time base are greater than those of DEM resolution, and at a fixed threshold the time to peak is independent of DEM resolution. According to the results of this study, one can deduce that DEM resolution and stream delineation threshold have significant effects on the performance of GIUH-based models, and researchers should be careful in using DEMs with different cell sizes and different thresholds.

References

[1] Akbari A, Abu Samah A, Othman F. Integration of SRTM and TRMM date into the GIS-based hydrological model for the purpose of ?ood modeling. Hydrol Earth Syst Sci 2012; 9: 4747–4775.

[2] Li J, Wong D. Effects of DEM sources on hydrologic applications. Comput Environ Urban Syst 2010; 34: 251–261.

[3] Chang KT, Tsai BW. The effect of DEM resolution on slope and aspect mapping. Cartogr Geogr Inf SCI 1991; 18: 69–77.

[4] Bian L, Walsh SJ. Scale dependencies of vegetation and topography in a mountainous environment of Montana. Prof Geogr 1993; 45: 1–11.

[5] Lam N, Quattrochi DA. On the issues of scale, resolution, and fractal analysis in the mapping sciences. Prof Geogr 1992; 44: 88–98.

[6] Kienzle S. The effect of DEM raster resolution on first order, second order and compound terrain derivatives. Transactions in GIS 2004; 8: 83–111.

[7] Lassueur T, Joost S, Randin CF. Very high resolution digital elevation models: do they improve models of plant species? Ecol Model 2006; 198: 139–153.

[8] McMaster KJ. Effects of digital elevation model resolution on derived stream network positions. Water Resources Res 2002; 38: 13-1–13-8.

[9] Hancock GR. The use of DEMs in the identification and characterization of catchment over different grid scales. Hydrol Process 2005; 19: 1727–1749.

[10] Chaubey I, Cotter AS, Costello TA, Soerens TS. Effect of DEM data resolution on swat output uncertainty. Hydrol Process 2005; 19: 621–628.

[11] Smith PA, Zhu AX, Burt JE, Stiles C. The effects of DEM resolution and neighborhood size on digital soil survey. Geoderma 2006; 137: 58–69.

[12] Pradahan NR, Ogden FR, Tachikawa Y, Takara K. Scaling of slope, upslope area, and soil water deficit: Implications for transferability and regionalization in topographic index modeling. Water Resources Res 2008; 44: W12421.

[13] Lin SC, Jing V, Chaplot XY, Zhang Z, Moore N, Wu J. Effect of DEM resolution on SWAT outputs of runoff, sediment and nutrients. Hydrol Earth Syst 2010; 7: 4411–4435.

[14] Nourani V, Zanardo S. Wavelet-based regularization of the extracted topographic index from high-resolution topography for hydro-geomorphic applications. Hydrol Process 2014; 28: 1345–1357.

[15] Nourani V, Roughani A, Gebremichael, M. TOPMODEL capability for rainfall-runoff modeling of the Ammameh watershed at different time scales using different terrain algorithms. J Urban Environ Eng 2011; 5: 1–14.

[16] Lee KT, Chang CH. Incorporating subsurface flow mechanism into geomorphology based IUH modeling. J Hydrol 2005; 311: 91–105.

[17] Lee KT, Yen BC. Geomorphology and kinematic wave based hydrograph derivation. J Hydraulic Eng 1997; 123: 73–80.

[18] Wooding RA. A hydraulic model for the catchment-stream problem. II. Numerical solutions. J Hydrol 1965; 3: 254–267.

[19] Chow VT. Handbook of Applied Hydrology. New York, NY, USA: McGraw-Hill; 1964.

[20] Usul N, Yılmaz M. A Pilot Project for Flood Analysis by Integration of Hydrologic Hydraulic Models and Geographic Information Systems. Ankara, Turkey: METU; 2002.

[21] Lee KT, Chen NC, Chung YR. Derivation of variable IUH corresponding to time-varying rainfall intensity during storms. Hydrol Sci. J 2008; 53: 323–327.

[22] Zhang WH, Montgomery DR. Digital elevation model grid size, landscape representation and hydrologic simulations. Water Resources Res 1994; 30: 1019–1028.

[23] Wolock DM, Price CV. Effects of digital elevation model map scale and data resolution on a topography-based watershed model. Water Resources Res 1994; 30: 3041–3052.